LA-UR-11-06575

Title:	Impact of Delayed Neutron Precursor Mobility in Fissile Solution Systems
Author(s):	Brian C. Kiedrowski
Intended for:	PHYSOR 2012 -- Advances in Reactor Physics April 15-20, 2012 Knoxville, TN, USA

PHYSOR 2012 Advances in Reactor Physics Linking Research, Industry, and Education
Knoxville, Tennessee, USA, April 15-20, 2012, on CD-ROM, American Nuclear Society, LaGrange Park, IL (2012)

IMPACT OF DELAYED NEUTRON PRECURSOR MOBILITY IN FISSILE SOLUTION SYSTEMS

Brian C. Kiedrowski
X-Computational Physics Division
Los Alamos National Laboratory
P.O. Box 1663, MS A143, Los Alamos, NM 87545
bckiedro@lanl.gov

ABSTRACT

A research version of the Monte Carlo software package MCNP6 is modified to incorporate advection and diffusion of delayed neutron precursors, resulting in the emission of delayed neutrons at locations different from the original fission sites. Results of two test problems, a pipe carrying flowing fissile solution and a sphere of fissile solution with precursor diffusion, show that the fission product mobility tends to perturb the fundamental mode, has a negative reactivity effect, and, perhaps most importantly, causes a decrease in the effective delayed neutron fraction.

Key Words: Monte Carlo, fluid dynamics, reactor safety

1. INTRODUCTION

A fraction of the neutrons produced in a reactor are introduced via neutron emission from the decay of certain fission products called delayed neutron precursors. In many systems, the delayed neutron precursors are not particularly mobile, and their neutrons are essentially born at the same location as the fission site. However, for systems that involve solutions with flows of fissile material or in high-temperature systems where the diffusivity of certain fission products is high, getting a correct estimate of the neutron distribution may require accounting for the transport of these fission products [1]. In fact, the FETCH software package (coupled thermal hydraulics and deterministic radiation transport) incorporates fission product precursor advection [2].

The equations including the mobility of delayed neutron precursors through advection and diffusion are given, and Monte Carlo techniques are developed that incorporate these precursor transport effects. The techniques are implemented in a research version of the Monte Carlo software package, MCNP6 [3,4]. Two test problems are presented: a reactor driven by a flowing uranyl nitrate solution through a reflector and a stationary sphere of uranyl nitrate solution with significant diffusion. The findings are that the steady state neutron distribution (fundamental mode) is affected, and there can be a impact to the effective delayed neutron fraction that can significantly reduce margins of reactor control.

2. THEORY & METHODOLOGY

2.1. Governing Equations

The time-dependent neutron transport equation may be written as a balance equation in simplified form as

$$\frac{1}{v}\frac{\partial\psi}{\partial t} + H\psi(\mathbf{r},\hat{\mathbf{\Omega}},E,t) = P\psi(\mathbf{r},\hat{\mathbf{\Omega}},E,t) + \sum_{i=1}^{M}\sum_{j=1}^{N}\frac{\chi_i^j(E)}{4\pi}\lambda_i^j C_i^j(\mathbf{r},t), \tag{1}$$

where v is the neutron speed, ψ is the neutron flux that is a function of the position $\mathbf{r}$, direction $\hat{\mathbf{\Omega}}$, energy E, and time t. H is the operator that includes the effects of streaming, collisions, and scattering, and P is the operator for prompt fission. The last term on the right is the emission of delayed neutrons from precursors. The subscript i is the index for the precursor group, of which there are M (typically $M = 6$ or $M = 8$). The superscript j denotes the isotope index, of which there are N. The emission spectrum for the precursor species i produced by a fission with isotope j is given by χ_i^j and the corresponding time decay constant is λ_i^j. Finally, $C_i^j(\mathbf{r},t)$ represents the concentration of the corresponding precursor at position $\mathbf{r}$ at time t.

In addition to the neutron transport equation there are $M \times N$ additional equations that must be solved to obtain each C_i^j. Typically, the equations are written as a rate equation where the time-rate of change of the precursor concentration is equal to production from fission minus losses from decay. The precursors may also undergo displacement from either advection or diffusion. Advection occurs in the presence of a bulk flow of a fissile fluid with a flow velocity vector field described by $\mathbf{u}(\mathbf{r})$. The precursors may also transport through atomic diffusion, which can be quantified by a diffusion coefficient $D_i^j(\mathbf{r})$.

Including the effects of advection and diffusion, the precursor rate equation is

$$\frac{\partial C_i^j}{\partial t} + \nabla\cdot\left[\mathbf{u}(\mathbf{r})C_i^j(\mathbf{r},t) - D_i^j(\mathbf{r})\nabla C_i^j(\mathbf{r},t)\right] = B_i^j\psi(\mathbf{r},\hat{\mathbf{\Omega}},E,t) - \lambda_i^j C_i^j(\mathbf{r},t). \tag{2}$$

Here B_i^j is the operator for production of delayed neutrons of a particular species from a given fissionable isotope.

The boundary conditions for Eq. (2) are typically one of four types. The first is continuity, where precursors at the boundary simply move from one region to another. The second is a sink, where a precursor that reaches the problem boundary is lost from the system. The third is a capture condition accounts for where a precursor may become captured by the boundary (e.g., a chemical reaction with the wall) such that its mobility is removed, but it still emits a delayed neutron at some future time. The fourth is a wall condition where no precursors may cross a boundary, and the precursor concentration current is zero there.

Eqs. (1) and (2) can be transformed into the k-eigenvalue formulation by the usual assertion of time independence, thereby setting the time derivatives to zero. The balance is retained by applying a factor of $1/k_{\text{eff}}$ to the right-hand side of Eq. (1). This factor, $1/k_{\text{eff}}$ is an eigenvalue, and the physical meaning of k_{eff} is the effective multiplication factor of the system. The other difference is that, unlike with the case where the precursors are immobile, $\lambda_i^j C_i^j$ can no longer be

simply substituted into the neutron transport equation, but must instead be obtained by solving the advection-diffusion equation. This can be done with standard finite difference techniques or, as is done here, solved by Monte Carlo by following the evolution of individual precursors.

2.2. Solution by Monte Carlo

The radiation transport equation is often "solved" with Monte Carlo techniques, and many production-level software packages are available for this end. Given a map of the fluid flow and diffusion coefficients, it is actually straightforward to extend the current Monte Carlo methods to account for the transport of delayed neutron precursors.

In the radiation transport simulation, when a precursor is produced from fission at time t_f, its lifetime τ is randomly sampled from an exponential distribution with parameter λ_i^j. Normally, a neutron appears at the same site as the fission event, just as a prompt neutron, except that its energy is sampled from a different distribution and its age is advanced to time $t_f + \tau$.

The advection and diffusion terms in Eq. (2) can be modeled as a Wiener process with a drift [5]. For generality of when the diffusion and fluid velocity field is not constant, the evolution in space of the precursor must be modeled using many time steps. The change in position of the simulated precursor with some position $\mathbf{r}_0$ at the start of the time step with interval Δt can be found by

$$\Delta \mathbf{r} = \mathbf{u}(\mathbf{r}_0)\Delta t + \mathbf{W}(\mathbf{r}_0), \tag{3}$$

where $\mathbf{W}$ is a random vector with a multivariate normal distribution normal distribution with zero mean and covariance matrix of $2D_i^j(\mathbf{r}_0)\Delta t$ along the diagonal and zero for the off-diagonal terms (no correlation between directions).

Should a simulated precursor hit the edge of a zone, some action must be taken depending upon the corresponding boundary condition. For a continuity condition, the precursor continues in the next zone. For a sink condition, the precursor simply disappears and no delayed neutron is produced. For a capture condition, the precursor simulation terminates, and a neutron is emitted at that location at time $t_f + \tau$. For a wall condition, the precursor is advanced to the boundary in a straight line along $\Delta \mathbf{r}$, Δt for the step is recalculated appropriately, and a new step in the precursor simulation is sampled.

The sampling of delayed neutron emission positions is the same regardless of whether the problem is a time-dependent or k-eigenvalue problem. While the k-eigenvalue equations are time independent, the time variable here can be thought of as a parameter used for sampling the positions where the delayed neutrons are emitted in the subsequent generation. This is analogous to how finite difference solutions are obtained for steady state advection-diffusion equations; the time variable is employed within the method, and the simulation terminates when equilibration is found.

3. TEST CASES

To understand the impacts of precursor mobility, the methods are implemented in MCNP6, simple models are constructed, and quantities such as k_{eff}, fission rates, and effective delayed neutron

fractions are computed (with adjoint weighting [6]). The two test cases are as follows: (1) A pipe of flowing uranyl nitrate solution through a neutron reflector and (2) a sphere of uranyl nitrate solution with no flow to illustrate the effect of diffusion.

These problems are neither verification nor validation of the method in a strict sense. Some verification may be performed in the loose sense by ensuring the results make physical sense, but there are no analytic solutions to compare. In this, it is, perhaps falsely, assumed that the methods and implementation are correct. Nonetheless, with this caveat understood, looking at results of specific test cases may still be useful to determine whether the effects are worth capturing.

3.1. Flowing Uranyl Nitrate Solution through a Reflector

A pipe is aligned along the x axis and contains uranyl nitrate solution (5% uranium concentration at 93.8 atom percent enrichment). The pipe consists of 316 stainless steel, and the inner radius of the pipe is 4 cm and is 0.5 cm thick. The problem begins at $x = -500$ cm. The reactor begins with an ORNL concrete wall 50 cm thick located at $x = -150$ cm, followed by a lead shield (doped with 100 ppm boron-10 for increased neutron absorption) starting at $x = -100$ cm. At $x = 0$ cm, there is a cylindrical nuclear-grade graphite reflector, 50 cm in diameter surrounding the pipe and extending until $x = 500$ cm; around the reflector is the lead shield. The lead shield continues from $x = 500$ to $x = 600$ cm, followed by a zone of ORNL concrete until $x = 650$ cm. The pipe extends to $x = 2000$ cm. The y and z extents of the geometry are 200 cm centered about the x axis. An illustration of the test case is given in Fig. 1.

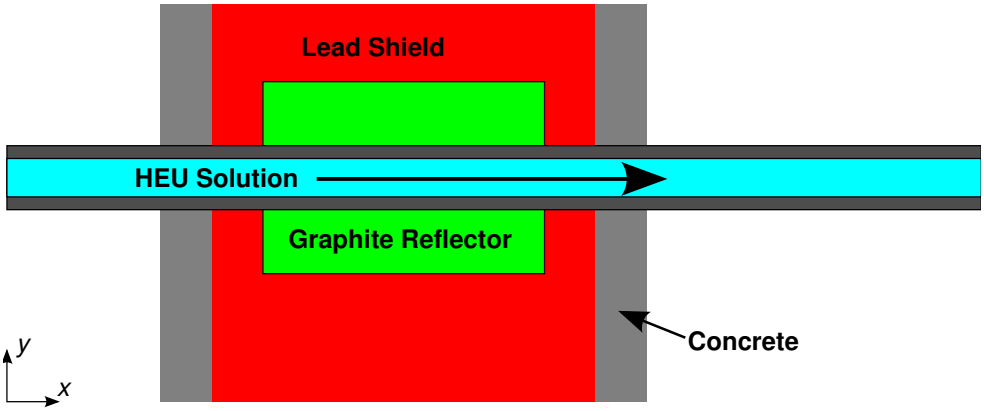

Figure 1: **Geometry of the Flowing Uranyl Nitrate Solution Case.**

The materials, except where stated, are taken form the PNNL Material Compendium [7]. All cross sections use ENDF/B-VII.1 nuclear data*. The assumption is that the precursors do not chemically interact with the pipe, so the pipe inner surface has a wall boundary condition. The boundary condition at the edge of the problem are sink conditions; precursors that reach either end of the pipe before undergoing decay are lost from the system.

Assuming laminar flow and a no-slip condition, the fluid only moves in the x direction with speed

*ENDF/B-VII.0 has known issues with the delayed neutron decay constant data and are generally not recommended for use should the λ_i^j be important.

profile as a function of radial distance [8] of

$$u_x(r) = u_{\max}\left[1 - \left(\frac{r}{R}\right)^2\right]. \tag{4}$$

Here, $u_{\max}$ is the maximal flow speed along the center (the input parameter) and contains factors such as the ratio of the pressure gradient to the fluid viscosity, R is the radius of the pipe, and r is the radial position from the x axis. By Eq. (4), the rate of precursor transport will be strongest for those born near the center of the pipe, and there is no transport (because of the no-slip condition) at the edge of the pipe.

MCNP6 calculations show the multiplication factor of the system with no fluid flow is $1.03177(9)$ [†] and the effective delayed neutron fraction is $0.00797(16)$. Various MCNP6 calculations are performed for various maximal flow rates (no diffusion), and results of the fission rate density (fundamental mode) and the effective delayed neutron fraction are obtained.

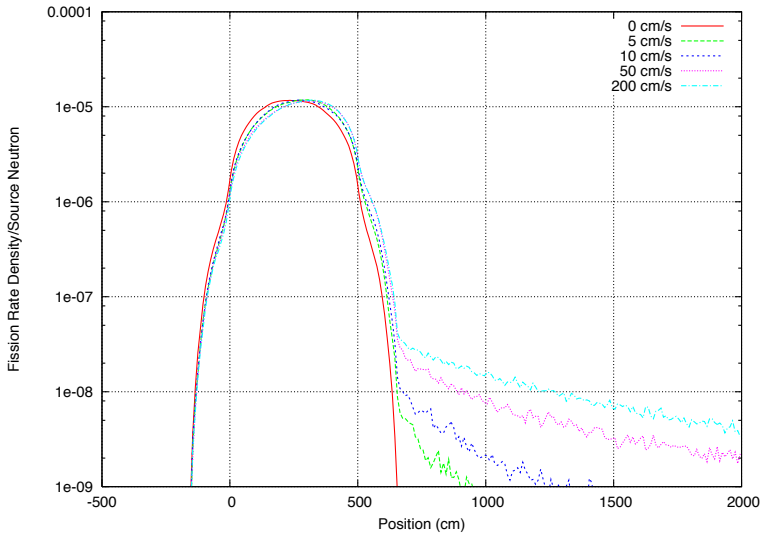

Figure 2: **Shift in fundamental mode for increasing flow rates.**

The fission rate density per source neutron as a function of x position is plotted in Fig. 2 for a few maximal flow rates ranging from no flow to 200 cm/s. For the no flow case, the fission rate is symmetric with a maximum around $x = 250$ cm, and drops off very quickly at the concrete wall. As the maximal flow increases, the fission rate density shifts in the positive x direction and has a noticeable tail that becomes longer and broader as the maximal flow increases, as expected. This means there is significantly more fission occurring in the pipe after the reactor than a static calculation would predict, having implications on shielding and cooling design. Additionally, the location of the maximum fission rate density shifts to the right by tens of centimeters (the 200 cm/s case has the maximum at about $x = 330$ cm, an 80 cm shift from the no flow case) in proportion to the maximal flow rate.

[†]The parenthetical number denotes the absolute, 1-σ statistical uncertainty (from Monte Carlo randomness) of the last digits of the quantity.

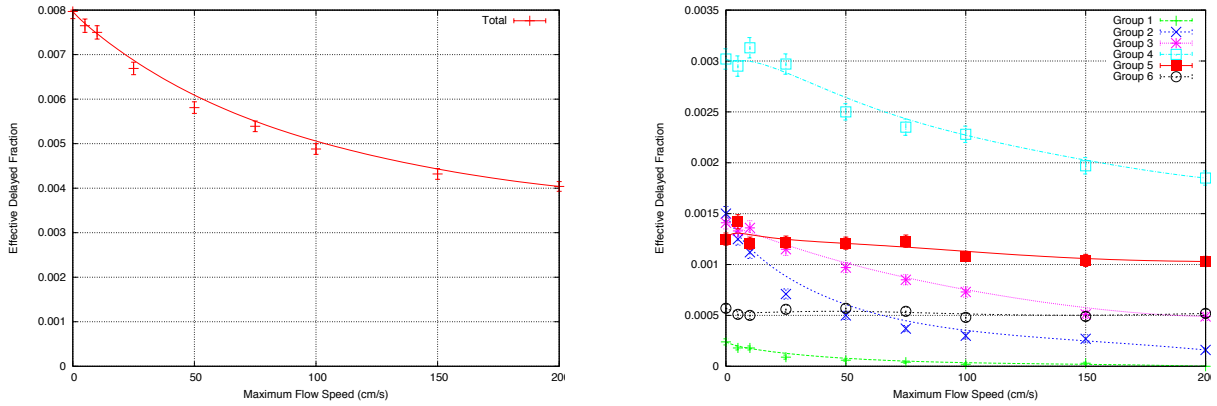

(a) (b)

Figure 3: **Changes in total (a) and individual components of (b) β_{eff} for various flow rates.**

Table I: **Uranium-235 Delayed Precursor Decay Data.**

Group	λ_i (s^{-1})	$t_{1/2}$ (s)
1	0.0133	51.98
2	0.0327	21.17
3	0.1208	5.74
4	0.3028	2.29
5	0.8495	0.82
6	2.8521	0.24

Fig. 3 shows the effective delayed neutron fraction β_{eff} and the $\beta_{i,\text{eff}}$ of each precursor group, as a function of the maximal flow rate, which shows a decrease in β_{eff} as the flow increases – to help interpret the results, the precursor decay constants and half-lives for uranium-235 (ENDF/B-VII.1) are given in Table I. This is because the precursors are being preferentially transported to regions that are less important or less able to drive a sustaining chain reaction, therefore the delayed neutrons have less of an impact on the criticality of the overall system. Since the system is near critical, k_{eff} is roughly decreased by the same amount, which must be compensated for in the design of the reactor. More concerning here is the decrease in β_{eff} (about a fifty percent degradation for a 200 cm/s maximal flow) because this decreases the control margin for the reactor, which has implications on the safety analysis of the design.

As the flow rate increases, the longer-lived precursors are swept out of the reactor before they can emit their neutrons. This is seen by the noticeable decrease in the $\beta_{i,\text{eff}}$ of the first four precursor groups as the maximum flow speed increases from 0 cm/s to 200 cm/s. Groups five and six have

much smaller or negligible changes because they tend to emit neutrons quickly enough such that the flow rates defined in this set of cases is insufficient to move them far enough out of the reactor to have serious impacts on their $\beta_{i,\text{eff}}$.

There is no observable impact on this system for all reasonable values of the diffusion coefficient.

3.2. Sphere of Uranyl Nitrate Solution

A sphere of uranyl nitrate solution is in a spherical 316 stainless steel tank with inner radius 9.0 cm and outer radius 9.2 cm. The materials and cross sections are the exact same as the previous case. There is no flow in the system, but diffusion effects are considered. Two boundary conditions are used: the wall condition where precursors are reflected when hitting the outer wall, and a capture case where precursors are held at the wall until they undergo decay. With either, no precursor is actually lost from the system, but the distribution of delayed neutron emission locations is altered. In the case of the wall condition, the distribution becomes more uniform, and in the capture condition, the distribution will be concentrated at the system edge.

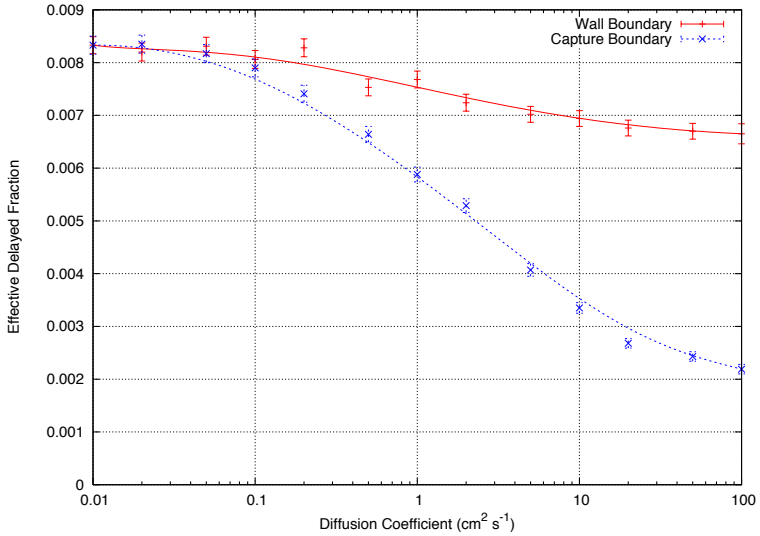

Figure 4: **Effective Delayed Neutron Fraction for Varied Diffusion Coefficients.**

Both should negatively impact the effective delayed neutron fraction, and this is illustrated in Fig. 4. The magnitude of the defect is far greater for the capture case since (about 70 pcm for $D = 1$ cm^2 s^{-1} with the wall boundary condition compared to about 250 pcm for the capture boundary condition), for large diffusion coefficients, all precursors end up at the boundary, and the delayed neutrons they emit are far less likely to establish a neutron population that propagates a sustained chain reaction. The wall boundary condition allows many of the delayed neutrons to be emitted closer to the center of system, and are therefore it is less likely for them or their possible progeny to leak out of the system – a stable fission chain becomes more likely.

The two boundary conditions represent the best and worst cases for a specified diffusion coefficient. Depending on the material properties of the boundary, some of the precursors will be

prone to chemically react with wall materials, forming a molecule that has a different diffusion coefficient (probably lower) than the free precursor atom. In the most extreme case, all precursors react with the wall, and the product of all the reactions have diffusion coefficients of zero; this leads to the greatest decrease in reactor control. With capture conditions, it is also possible for β_{eff} (and, by extension, k_{eff}) to increase if the capturing boundaries are prone to concentrating precursors in regions of high importance.

An important point here is that most materials have a mass diffusion coefficient much smaller than the range tested. This implies that for most systems, diffusion can be safely neglected. Exceptions may be high temperature systems where the fission products may encounter porous media; this situation is generally avoided in the system design (e.g., high-temperature gas-cooled reactors) for reasons of avoiding fission product release, and not reactivity concerns.

4. CONCLUSIONS & FUTURE WORK

A Monte Carlo method for incorporating the advection and diffusion of delayed neutron precursors is implemented in a research version of MCNP6. Two test problems are used to demonstrate the impact of both effects, and it appears (as expected) that advection is typically dominant. Advection may cause a significant shift in the fundamental mode should flow rates of fissile solution be high enough. Also, there may be a significant decrease in β_{eff}, the effective delayed neutron fraction, should the transport processes be sufficient to move enough delayed precursors out of important regions (regions of high adjoint flux).

Further work would investigate efficient and production-level mechanics of incorporating a realistic fluid flow map from a computational fluid dynamics package into MCNP. This would allow for the analysis of more realistic and relevant systems such as molten salt reactors, where continuous-energy Monte Carlo may be a useful tool for quantifying the reactivity effects. Also, the presence of turbulent flows and vortexes may create hot spots of delayed neutron emission that should be quantified in a system design – this possible effect needs to be investigated. Finally, the methodology is not just limited to delayed neutron precursors, but may be done for any fission product. The transport of xenon-135 may create a noticeable impact on power shapes for fluid or porous systems, and these techniques may be useful to investigate these effects as well.

ACKNOWLEDGMENTS

This work was performed with support of the US DOE/NNSA Nuclear Criticality Safety Program. Special thanks to Dr. Michael Fensin at LANL for his discussions that motivated this work.

REFERENCES

[1] G. R. Keepin, *Physics of Nuclear Kinetics*, Ch. 4, Addison-Wesley Publishing Company, Inc., Reading, MA, USA (1965).

[2] C. C. Pain, C. R. E. de Oliveira, A. J. H. Goddard, A. P. Umpleby, "Transient Criticality in Fissile Solutions – Compressibility Effects," *Nucl. Sci. & Engr.*, **138**, pp. 78-95 (2001).

[3] J. T. Goorley, et. al., "Initial MCNP6 Release Overview," Los Alamos National Laboratory Report, LA-UR-11-01766 (2011).

[4] X-5 Monte Carlo Team, "MCNP A General N-Particle Transport Code, Version 5," Vol. I, Los Alamos National Laboratory Report, LA-UR-03-1987 (2003).

[5] G. R. Grimmett, D. R. Stirzaker, *Probability and Random Processes, 3rd Ed.*, Ch. 13, Oxford University Press, Oxford, UK (2001).

[6] B. C. Kiedrowski, F. B. Brown, P. P. H. Wilson, "Adjoint-Weighted Tallies for k-Eigenvalue Calculations with Continuous-Energy Monte Carlo," *Nucl. Sci. & Engr.*, **168**, pp. 226-241 (2011).

[7] R. G. Williams, C. J. Gesh, R. T. Pugh, "Compendium of Material Composition Data for Radiation Transport Modeling," Pacific Northwest National Laboratory Report, PNNL-15870 (2006).

[8] R. B. Bird, W. E. Stewart, E. N. Lightfoot, *Transport Phenomena, 2nd Ed.*, John Wiley & Sons, Inc., New York, NY, USA (2007).